Published in final edited form as:

Acta Biomater. 2017 August ; 58: 302–311. doi:10.1016/j.actbio.2017.06.016.

Chondrogenesis of Human Bone Marrow Mesenchymal Stem Cells in 3-Dimensional, Photocrosslinked Hydrogel Constructs: Effect of Cell Seeding Density and Material Stiffness

Aaron X. Sun[1,2,3], **Hang Lin**[1], **Madalyn R. Fritch**[1,3], **He Shen**[1,5], **Pete G. Alexander**[1], **Michael DeHart**[4], and **Rocky S. Tuan**[1,3,*]

[1]Center for Cellular and Molecular Engineering, Department of Orthopaedic Surgery, Pittsburgh, PA, USA

[2]Medical Scientist Training Program, University of Pittsburgh School of Medicine, Pittsburgh, PA, USA

[3]Department of Bioengineering, University of Pittsburgh Swanson School of Engineering, Pittsburgh, PA, USA

[4]Department of Biology, University of Pittsburgh Dietrich School of Arts and Sciences, Pittsburgh, PA, USA

[5]Key Laboratory of Nano-Bio Interface, Division of Nanobiomedicine, Suzhou Institute of Nano-tech and Nano-bionics, Chinese Academy of Sciences, China

Abstract

Three-dimensional hydrogel constructs incorporated with live stem cells that support chondrogenic differentiation and maintenance offer a promising regenerative route towards addressing the limited self-repair capabilities of articular cartilage. In particular, hydrogel scaffolds that augment chondrogenesis and recapitulate the native physical properties of cartilage, such as compressive strength, can potentially be applied in point-of-care procedures. We report here the synthesis of two new materials, [poly-L-lactic acid/polyethylene glycol/poly-L-lactic acid] (PLLA-PEG 1000) and [poly-D,L-lactic acid/polyethylene glycol/poly-D,L-lactic acid] (PDLLA-PEG 1000), that are biodegradable, biocompatible (>80% viability post fabrication), and possess high, physiologically relevant mechanical strength (~1,500 to 1,800 kPa). This study examined the effects of physiologically relevant cell densities (4, 8, 20, and 50 × 10^6/mL) and hydrogel stiffnesses (~150kPa to ~1,500 kPa Young's moduli) on chondrogenesis of human bone marrow stem cells incorporated in hydrogel constructs fabricated with these materials and a previously characterized PDLLA-PEG 4000. Results showed that 20 × 10^6 cells/mL, under a static culture condition, was the most efficient cell seeding density for extracellular matrix (ECM) production on the basis of hydroxyproline and glycosaminoglycan content. Interestingly, material stiffness did not significantly affect chondrogenesis, but rather material concentration was correlated to chondrogenesis with increasing levels at lower concentrations based on ECM production, chondrogenic gene expression, and histological analysis. These findings establish

[*]**Correspondence:** Dr. Rocky S. Tuan, Center for Cellular and Molecular Engineering, Department of Orthopaedic Surgery, University of Pittsburgh School of Medicine, Pittsburgh, PA, 15219, USA. rst13@pitt.edu.

optimal cell densities for chondrogenesis within three-dimensional cell-incorporated hydrogels, inform hydrogel material development for cartilage tissue engineering, and demonstrate the efficacy and potential utility of PDLLA-PEG 1000 for point-of-care treatment of cartilage defects.

Graphical abstract

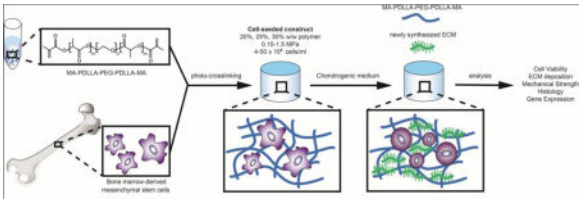

Keywords

bone marrow stem cells; cartilage tissue engineering; biomaterial scaffold; PDLLA-PEG; PLLA-PEG

1. Introduction

Cartilage tissue possesses limited potential for self-repair, and damage resulting from various disease processes, aging, or trauma ultimately leads to the formation of a persistent cartilage defect and the onset of osteoarthritis (OA).[1] OA is a degenerative joint disease that affects approximately 27 million people in the U.S. each year and it places a heavy burden on society at a cost of approximately $89.1 billion yearly.[2,3] Although the pathogenesis of OA is not fully understood, age and body habitus contribute heavily to the development of OA, and with an ever-aging population suffering from increasing rates of obesity, methods towards addressing and alleviating the burden of this debilitating disease are a necessity.

Traditional treatment options aimed at resolving the osteochondral defect in OA have provided limited success with each bearing their own inadequacies.[4] The use of an osteochondral allograft provides native tissue that can be used to fill the defect, but it has the potential for immune rejection, disease transmission, and infection. Microfracture stimulates endogenous repair by a small fracture injury to the bone, but it can result in the formation of mechanically inferior fibrocartilage instead of native hyaline cartilage, thereby requiring a second intervention. Total joint arthroplasty, which is usually reserved for severe cases of OA, increases mobility but eliminates the potential for biological joint repair and requires a major surgery, which may not be an option for many patients.[5,6] In addition, this repair has limited lifespan in young patients, thus necessitating multiple surgeries over a lifetime. Given the respective limitations of these techniques, new approaches towards treating OA are actively being pursued.

Recently, regenerative medicine strategies using autologous cells, biomaterial scaffolds, and growth factors have garnered significant interest as potential routes to repair the osteochondral defect.[1,7] One set of techniques, autologous chondrocyte implantation (ACI) and matrix-induced ACI (MACI), involve harvesting healthy chondrocytes from non-weight bearing regions of articular cartilage and expanding the chondrocytes *in vitro* for re-

implantation with or without cell seeding onto a biomaterial extracellular matrix (ECM).[8,9] While such techniques utilizing mature adult cells offer a viable regenerative approach, they are constrained by lengthy cell expansion times, the potential for de-differentiation of chondrocytes during the expansion period, and contamination.[10] Another promising avenue towards obtaining mature chondrocytes involves the use of adult mesenchymal stem cells (MSCs), which have the ability to differentiate into a variety of lineages, including chondrocytes.[11] Bone marrow derived stem cells (BMSCs) in particular are of great interest for they are one of the most extensively studied MSCs, and intra-articular injections of BMSCs have been reported to reduce osteoarthritic pain, improve joint mobility, and slow progressive osteoarthritic degeneration.[12–14] As such, regeneration in OA employing BMSCs is an attractive alternative to currently applied ACI procedures.

The ideal scaffold should mimic the mechanical properties of cartilage, degrade as cells secrete their own extracellular matrix (ECM), and provide an environment conducive to cell survival and maintenance of a chondrocyte lineage. Many biomaterials have been developed that allow for live cell incorporation, but none adequately fulfill all the requirements of an ideal scaffold.[15–17] Recently, we reported the use of a water soluble methacrylated polyethyleneglycol-poly-D,L-lactide (mPDLLA-PEG) biodegradable polymer for live cell scaffold fabrication that possessed high mechanical strength (~780 kPa).[18] While this scaffold possessed physiologically relevant mechanical strength on fabrication, we found that after 4 weeks the strength of the cell-seeded scaffold had degraded drastically (~240 kPa). This finding implies that ECM deposition by the encapsulated cells failed to provide sufficient mechanical reinforcement to the scaffold. Augmenting this ability is thus necessary, for example by varying factors such as cell density and material properties, both of which may affect ECM production, deposition, and organization. Indeed, for cells incorporated in hyaluronic acid and alginate 3D scaffolds increasing levels of matrix organization and deposition were seen with increasing concentrations of initial cell seeding density up to approximately 20×10^6 cells/mL.[19–22] On the other hand, an important material property, stiffness, is also known to play a part in determining stem cell differentiation into different lineages on both 2D and 3D substrates.[23–29] For 2D surface-seeded chondrocytes, mechanically matching scaffolds allowed for retention of rounded chondrocyte morphology and higher ECM production than counterparts with lower stiffnesses.[30] However, this is contrasted by BMSC behavior in 3D hyaluronic acid hydrogels where higher crosslinking densities and moduli led to a decrease in ECM production.[31,32] Given these observations, optimization of cell concentration and material stiffness is likely to be critical for enhanced chondrogenesis in live cell incorporated scaffolds that possess physiologically relevant mechanical properties.

In this study, we report the development of two new biomaterials, PDLLA-PEG 1000 and PLLA-PEG 1000, which are low molecular weight versions of our previously reported material, PDLLA-PEG 4000 (the terminal number indicates the molecular weight of the PEG chain) for use in live cell 3D incorporation. These new polymers exhibit properties of biodegradability and biocompatibility similar to those of the previous PDLLA-PEG 4000, but they possess mechanical properties that are much higher due to increased crosslinking density. Using these 3D materials, for the first time we probe the cellular efficiency of ECM production with varying cell densities and the effects of modulating material stiffness on

chondrogenesis on a physiologically relevant scale (~150 kPa to 1500 kPa Young's modulus) in static cultured human BMSC (hBMSC) incorporated hydrogels. Our results should inform cell seeding protocols and the development of mechanically appropriate scaffolds for point-of-care articular cartilage tissue engineering.

2. Materials and Methods

All chemicals were purchased from Sigma Aldrich (St. Louis, MO, USA) unless otherwise specified.

2.1 Human Bone Marrow Stem Cell Isolation

hBMSCs were isolated from the femoral heads of patients undergoing total joint arthroplasty with IRB approval (University of Washington and University of Pittsburgh), and cultured and expanded as previously described.[33] Briefly, bone marrow was flushed out from the trabecular bone of the femoral neck and head using an 18-gauge needle and re-suspended in Dulbecco's Minimal Essential Medium (DMEM). The suspension was filtered through a 40 μm strainer and the flow-through was centrifuged at 300*g* for 5 min. After the supernatant was discarded, the cell pellets were re-suspended using growth medium (GM, α-MEM containing 10% fetal bovine serum (FBS, Invitrogen), 1X antibiotics-antimycotic (Ampicillin 100 units/mL, Streptomycin 100 μg/mL, Amphotericin B 250 ng/mL), and 1.5 ng/mL FGF-2 (RayBiotech, Norcross, GA)), and then plated into 150 cm^2 tissue culture flasks at a density of 20,000-40,000 nucleated cells/cm^2, and medium was changed every 3 to 4 days. Once 70% to 80% confluence was reached, cells were passaged. All experiments were performed with passage 4 (P4) hBMSCs except the cell concentration experiments, which were performed with passage 3 (P3) hBMSCs. All cells used in this study were pooled from three patients: 58 y/o female, 62 y/o female, and 69 y/o male.

2.2 Synthesis of Methacrylated PDLLA-PEG 4000, PDLLA-PEG 1000, and PLLA-PEG 1000

Preparation of mPDLLA-PEG 4000 was performed as described by Seck et al.[34] Briefly, 50 g of PEG (4 kDa molecular weight) was placed into a 250 mL beaker and subjected to 600 W microwave irradiation for 3 min. Subsequently, 3.5 g (2.80 mL) of stannous octoate [$Sn(Oct)_2$] was added to the molten PEG followed by addition of 7.2 g D,L-lactide. The mixture was briefly swirled to mix the contents and then subjected to 600 W microwave irradiation for 1 min. The initial PDLLA-PEG 4000 polymer was precipitated in 500 mL cold isopropanol and dried under vacuum for 2 days. The dry polymer was placed into a dry 500 mL round bottom flask and dissolved in 100 mL dichloromethane (DCM) followed by addition of three equivalents of trimethylamine (TEA, ~5.25 mL) and three equivalents of methacrylic anhydride (MA, ~5.60 mL). The reaction mixture was placed under Argon gas and allowed to stir at room temperature for 7 days. After completion of the reaction, the mixture was precipitated into diethyl ether. For further purification, the macromere was re-dissolved in minimal amounts of chloroform and re-precipitated in diethyl either.

Preparation of mPDLLA-PEG 1000 and mPLLA-PEG 1000 was carried out similarly as above, except PEG with 1 kDa molecular weight was used in the synthesis and L-lactide was used in place of D,L-lactide for the latter synthesis. In addition, the two precipitation steps

(isopropanol and diethyl ether) included 1 hour of cooling at −20 °C after initial precipitation to allow for the product to completely precipitate out.

2.3 Synthesis of Photoinitiator LAP

The visible-light sensitive initiator lithium phenyl-2,4,6-trimethylbenzoylphosphinate (LAP) was synthesized as described by Fairbanks et al.[35]

2.4 Fabrication of Live Cell Incorporated Constructs

Solutions of polymer and LAP were prepared in 50 mL tubes with 0.3% w/v photoinitiator and either 30%, 25%, or 20% w/v polymer. These concentrations were chosen to yield a range of Young's moduli from ~150 kPa to ~1500 kPa. For instance, the preparation of mPDLLA-PEG 1000 (30% w/v) and LAP (0.3% w/v) was carried out as follows: 12g mPDLLA-PEG 1000 was placed in a 50 mL tube followed by addition of Hanks Balanced Salt Solution (HBSS) close to the 40 mL mark. The solution was subsequently titrated to pH 7.4 with 10 N NaOH and adjusted to 40 mL using HBSS followed by addition of 120 mg LAP (0.3% w/v).

hBMSCs were pelleted by centrifugation, and the supernatant was completely removed. The appropriate amount of polymer solution was added on top of the pellets and mixed with cells thoroughly by pipetting up and down 20 times for a final concentration of either 4×10^6, 8×10^6, 20×10^6, or 50×10^6 cells/mL. After the bubbles were removed by aspiration, the cell-polymer solution was pipetted to fill multiple circular 5 mm diameter × 2 mm height molds punched out of silicone rubber. Subsequently, a glass coverslip was placed over the molds to ensure flat cylindrical structures. Following this, a visible light source supplying wavelengths of 395 nm (7202UV395, LEDWholesalers) was used to cure the polymers for 2 minutes.

The completed constructs were cultured in chondrogenic medium [DMEM with 1% L-alanyl- L-glutamine (GlutaMAX), 55 μM sodium pyruvate, 1X antibiotic-antimycotic, 1% insulin-transferrin-selenium (ITS)(Invitrogen, Carlsbad, CA, USA), 10 ng/mL transforming growth factor-β3 (TGF-β3; PeproTech, Rocky Hill, NJ, USA), 100 nM dexamethasone, 50 μM L-ascorbic acid 2-phosphate, and 23 μM L-proline]] for up to 8 weeks.

2.5 Degradation Test and Mechanical Testing

The extent of degradation of polymers is determined indirectly, by measuring the mechanical property of scaffolds.[20] Cell-free scaffolds fabricated as described above were immersed in 4 mL HBSS supplemented with 1X antibiotic-antimycotic and maintained in a cell culture incubator at 37 °C. HBSS was changed every 3 days.

Mechanical testing of scaffolds was conducted with a mechanical tester (Bose Electroforce model 3230 Series II). Briefly, the cylindrical scaffolds were placed between the compressive motor and the load cell and subjected to 10% compression (0.2 mm) at 0.01 mm/s. The stress-strain curve was then plotted, and the linear area was used to calculate the compressive modulus of the scaffolds.

2.6 Live/Dead Staining

At days 1 and 7 post fabrication, cell viability was assessed with the Live/Dead viability/cytotoxicity kit (Invitrogen) as examined by epifluorescence microscopy following the product manual. The percentage of live cells was calculated by counting the number of live green cells divided by the total (green and red cells together) in cross-sections that spanned both the center and border of the constructs. Clusters of cells were counted to the best visual discrimination of single cells. Images were captured with an inverted microscope (Olympus CKX41, Japan) equipped with a Leica DFC 4300 camera.

2.7 Sulfated Glycosaminoglycan (sGAG) and Hydroxyproline Quantification

Cartilage ECM deposition was quantified by measuring sGAG and total collagen production. Constructs were homogenized and then digested for 18 h in 700 μl/construct of a papain solution (125 μg/ml papain, 50 mM sodium phosphate buffer, 2 mM N-acetyl cysteine (Sigma), pH 6.5). An aliquot of the digest was assayed for sGAG content using the Blyscan kit (Accurate Chemical & Scientific Corp, Westbury, NY) according to the manufacturer's instruction. Another aliquot of the digest was assayed for DNA content using the QuantiT PicoGreen dsDNA Assay Kit (Invitrogen).

A third aliquot was used to quantify collagen deposition by measuring hydroxyproline levels using a modified hydroxyproline assay with bovine collagen type I as a standard. Briefly, 200 μl of each sample and standard were hydrolyzed with 200 μl of 4 N sodium hydroxide (Fisher) at 121 °C for 20 min. 200 μl of 4N HCl (Fisher) was added and the solution was titrated to a neutral pH. 1.2 mL of chloramine-T solution (Sigma) (14.1 g/L chloramine-T, 50 g/L citric acid, g/L sodium acetate trihydrate, 34 g/L NaOH, 0.21 M acetic acid) was incubated at room temperature for 20 min. Then, 1.2 mL of 15 g/L p-dimethylaminobenzaldehyde in 2:1 isopropanol:perchloric acid was added and the solution was placed in a 60 °C water bath for 20 min. Finally, 200 μl of each sample in triplicate was added into a 96 well plate and absorbance was read at 550 nm.

2.8 Analysis of Gene Expression by Real Time Reverse Transcription PCR (RT-PCR)

Total RNA of the cells within constructs was isolated by homogenizing in TRIZOL reagent (Invitrogen) and purified using RNeasy Plus Mini Kit (Qiagen, Germantown, MD, USA). Reverse transcription was achieved using SuperScript® VILO™ cDNA Synthesis Kit (Invitrogen) according to the manufacturer's protocol. Real-time PCR was performed using the SYBR Green Reaction Mix (Applied Biosystems, Foster City, CA, USA) with a StepOne-Plus thermocycler (Applied Biosystems). Gene expression levels of Sox 9, collagen types II and X, aggrecan and matrix metalloproteinase 13 (MMP13) were analyzed. All sample values were normalized to ribosomal protein L13a (RPL13A) using the $2^{-\Delta\Delta Ct}$ method.

2.9 Histology

Whole constructs were fixed in 10% neutral buffered formalin (Fisher Scientific, Pittsburgh, PA) for 1 day, dehydrated, paraffin-embedded, and 10 μm sections were prepared. Staining with Safranin O/Fast Green and Alcian Blue/Fast Red was used to detect sGAG and proteoglycan deposition.

2.10 Transferrin Perfusion

Cell-seeded constructs composed of 30% PDLLA-PEG 4000 were fabricated as described above. These were cultured in chondrogenic medium containing Transferrin-546 nm (Invitrogen) at 60 μg/ml for 14 days. Constructs were then fixed in 4% paraformaldehyde overnight at 4°C, equilibrated in sucrose, and embedded in optimal cutting temperature (OCT) compound. These were then sectioned at 50 μm.

2.11 Statistical Analysis

All data were expressed as mean ± standard deviation and statistical analysis was performed using either two-way independent analysis of variance (ANOVA) or two-way independent multivariate analysis of variance (MANOVA) followed by Tukey's HSD post hoc testing. A threshold of $p < 0.05$ was used to determine statistical significance.

3. Results

3.1 Mechanical testing and degradation analysis

Figure 1 shows the mechanical properties of PDLLA-PEG 4000, PDLLA-PEG 1000, and PLLA-PEG 1000 over 28 days in HBSS. Due to the presence of ester bonds between lactide molecules and PEG, the polymers are expected to degrade through hydrolytic cleavage (Seck et al, 2010). The compressive moduli of the scaffolds decreased steadily over time, with a $p<0.001$ between each time point within each group, except for between days 21 and 28 where the rate of change slowed. Statistically significant differences were also found in group and concentration effects with regard to mechanical strength ($p<0.001$). The new materials, PDLLA-PEG 1000 and PLLA-PEG 1000, were significantly stronger than PDLLA-PEG 4000, as evidenced by a 3- to 4- fold higher compressive modulus at all time points. In addition, the low molecular weight scaffolds did not swell in HBSS, likely contributing to their strength.

3.2 Cell viability assessment in new materials

For the new materials, PDLLA-PEG 1000 and PLLA-PEG 1000, cell viability remained high between the post-fabrication period and day 7 with cell viability >85% in all groups at day 7 (Figure 2). The viability did not change significantly between the different concentrations of polymer, indicating that at 20×10^6 cells/mL adequate nutrient diffusion was achieved at all concentrations and that the materials were biocompatible.

3.3 Determining optimal cell density

Cells seeded in 30% PDLLA-PEG 4000 at varying concentrations all exhibited a significant difference in compressive moduli between 4 and 8 weeks after fabrication (Figure 3A, $p<0.05$), but mechanical strength was neither increased nor maintained within any group. Examination of DNA levels showed significant differences between all groups except the 20×10^6 cells/mL and 50×10^6 cells/mL groups ($p=0.178$) (Figure 3B). Total sGAG and hydroxyproline deposition was significantly higher in the 20×10^6 cells/mL group when compared to 4 and 8×10^6 cells/mL ($p<0.001$), but was not significantly different from 50×10^6 cells/mL (Figures 3C, 3E). However, when normalized to number of cells originally

seeded in the constructs, the 20×10^6 cells/mL group had significantly higher sGAG deposition than all other groups ($p<0.001$) (Figures 3D, 3F). Safranin O and Alcian Blue staining demonstrate strong GAG deposition by both 20 and 50×10^6 cells/mL groups, with the former showing uniform staining and the latter showing weaker central staining (Figures 4A-4D). To evaluate whether the non-uniform pattern of chondrogenesis could be related to accessibility to TGF-β3, fluorescently labeled transferrin (ITS - yellow) was added to the culture medium as a tracer of similar molecular size to TGF-β3 to assess its diffusion through the scaffold at different cell densities. Fluorescence microscopy revealed that at higher cell density, ITS staining was limited to the periphery of the scaffold (Figure 4F), while at lower cell density the ITS uptake was more uniform (Figure 4E). Sections were taken at approximately the center of each scaffold.

3.4 Effect of material stiffness on chondrogenesis

Compressive moduli of PDLLA and PLLA-PEG 1000 were significantly higher at all concentrations and time points than corresponding PDLLA-PEG 4000 ($p<0.001$) (Figure 5A). However, compressive moduli were not maintained over the 28-day culture period. DNA content was significantly higher in the PDLLA-PEG 4000 groups across the 3 concentrations than in the other low molecular weight groups ($p<0.001$), most likely due to the swelling of the scaffold which provided for more space for cell proliferation (Figure 5B). Due in part to this higher cell number, the group effects for total levels of sGAG and hydroxyproline were significantly higher for PDLLA-PEG 4000 *versus* PDLLA and PLLA-PEG 1000 ($p<0.005$) (Figure 5C, 5E). However, when calculated based on DNA content there was no significant difference in the group effects of sGAG/DNA and hydroxyproline/DNA for PDLLA-PEG 4000 *versus* PDLLA-PEG 1000 ($p>0.5$ for both) (Figure 5D,5F). In all measures of ECM production, PLLA-PEG 1000 was significantly lower than either of the other two groups ($p<0.001$)(Figures 5C-5F). In addition, there was a significant polymer concentration effect for sGAG/DNA and sGAG/construct, with $p<0.05$ for 20% *versus* 25%, 25% *versus* 30%, and 20% *versus* 30%. The only exception to this was in sGAG/DNA, with $p=0.06$ for 25% *versus* 30%. (Figures 5C, 5D).

The influence of polymer concentrations on chondrogenic gene expression across the different groups is shown in Figure 6. Overall, there was a significant polymer concentration effect for PLLA-PEG 1000 for all combinations of concentrations in all genes tested ($p<0.05$). The exceptions to this in the PLLA-PEG 1000 group were for collagen type X (20% *versus* 25%, $p=0.286$) and MMP13 (25% *versus* 30%, $p > 0.5$). Conversely, PDLLA-PEG 1000 exhibited significant differences only between 25% and 30% and PDLLA-PEG 4000 in general contained no significant differences between groups. The one exception in the PDLLA-PEG 4000 group was for 20% *versus* 30% in collagen type II ($p=0.045$). Lastly, multivariate analysis of PDLLA-PEG 4000 *versus* PDLLA-PEG 1000 to determine differences in chondrogenic potential revealed no significant differences across all genes except MMP13, which had a $p=0.027$.

Histological analysis of ECM production using Alcian Blue/fast red staining is shown in Figure 7. Strong sGAG deposition is seen across all polymer concentrations in the PDLLA-PEG 4000 group with decreasing staining as concentration of material was increased

(Figures 7A-C). PDLLA-PEG 1000 group exhibited a similar trend of strong staining, which decreased with increasing polymer concentration (Figures 7D-F). In contrast, cells exhibit weak staining across all three polymer concentrations in the PLLA-PEG 1000 group (Figures 7G-I). The histological findings thus correlated well with the gene expression data, with PLLA-PEG 1000 scaffolds showing significant differences in gene expression levels of chondrogenic markers when compared to PDLLA-PEG 1000.

4. Discussion

The goal of this study was to identify and characterize a candidate biomaterial scaffold that is able to support chondrogenic differentiation of seeded hBMSCs, and possesses a biodegradability profile sufficient to mimic the mechanical properties of the native cartilage tissue. As a control, the previously characterized material, PDLLA-PEG 4000, was used. We identified PDLLA-PEG 1000 as a material that possesses mechanical properties in the range of native articular cartilage, and demonstrated both high cell viability and chondrogenic potential of seeded hBMSCs within the material construct. We found that the optimal cell seeding density for ECM deposition in this material was 20×10^6 cells/mL due to limited nutrient diffusion above those concentrations, and interestingly, we also observed that hBMSC chondrogenesis within this material was dependent on material concentration, not material stiffness. These findings point to the potential utility of this material in point-of-care articular cartilage repair and inform future material development.

A point-of-care engineered cartilage construct ideally possesses mechanical properties similar to native cartilage at the time of fabrication.[1] Towards this end, the new low molecular weight polymers possessed much higher moduli than PDLLA-PEG 4000, presumably due to the increased number of crosslinking chains. Indeed, this increase in toughness of methacrylate networks corresponding to higher crosslinking density has been previously described.[36] Interestingly, PLLA-PEG 1000 displayed higher moduli than PDLLA-PEG 1000 at the same concentrations despite having a similar chemical composition (as shown in Figure 1), but we hypothesize that this can be explained by lower levels of hydrolysis, which is a known degradation mode for these networks,[37] in the former during the pH neutralization step of the material preparation (see **section 2.5**). Degradability has been shown to be an important component of successful remodeling,[38–40] and these new materials possessed similar degradation rates to PDLLA-PEG 4000 likely due to all materials having the same ratio of hydrolyzable lactide to PEG moieties.

With materials covering a wide range of mechanical stiffnesses, the optimal constructs for chondrogenesis in static culture were assessed by examining the effect of cell concentrations on ECM production and mechanical properties. Our results showed that 20×10^6 cells/mL loading density allowed for the most efficient production of ECM per cell (Figure 3). Interestingly, this concentration is similar to those reported to be optimal in softer hydrogels such as hyaluronic acid[19,20,22]. We also observe that the DNA content of 20 and 50×10^6 cells/mL groups are the similar at 4 and 8 weeks, which we hypothesize is due to cell death in the latter. A combination of two factors is potentially at play: saturation of cells per unit volume in the confined space of the construct, and limitation in cell support by nutrient diffusion through the scaffold in static culture. Nutrient diffusion has been implicated as a

limiting factor for ECM production, as Mauck et al. demonstrated that increased nutrient diffusion through mechanical stimulation allowed for higher levels of ECM deposition at high cell densities.[25,26] Indeed, at 50×10^6 cells/mL, the periphery of the scaffold showed strong matrix GAG staining with both Alcian blue and Safranin O compared to the center in contrast to the uniform staining seen in the 20×10^6 cells/mL group. This region-dependent characteristic of MSC chondrogenesis has been demonstrated by Farrell et al. and is in accordance with our findings.[41] Results in Figures 4E and 4F suggest that this phenomenon may be due to the lower cell density allowing for higher diffusion of transferrin, a molecule of similar size to TGFβ3, through the entire scaffold. It is noteworthy that all hydrogel constructs were cultured sitting undisturbed on flat surfaces (the bottom of a six-well tissue culture plate) with the minimum amount of medium needed to cover the top surface, thus little to no diffusion occurred from the top/bottom and most diffusion occurred along the lateral edge of the constructs.

Another factor known to influence stem cell behavior is matrix stiffness, with stiffer matrices promoting osteogenesis and softer ones driving cell fate toward adipogenesis.[23–29] However, how stiffness affects MSC chondrogenesis in degradable 3D networks within the physiological range of cartilage stiffness has not been reported. With the optimal cell concentration for static culture established, we next studied the influence of scaffold mechanical property on ECM production (Figure 5) and gene expression (Figure 6) at a cell concentration of 20×10^6 cells/mL. Strikingly, on the basis of ECM deposition, we found that mechanical stiffness is unlikely to be the driving factor between the differences in ECM production, but rather it is the concentration of the polymer used to create the hydrogel that seems to dictate the biological response. Specifically, the free space (as a function of concentration) available in the scaffold seems to drive the ability of the cells to produce ECM. This can be clearly seen in the case of gene expression in PLLA-PEG 1000 (Figure 6), where the expression levels of ECM related genes (Sox9, Col II, Aggrecan, Col X) are increasingly downregulated as concentration increases, whereas matrix catabolic gene MMP13 is upregulated with increasing concentration. We also observe that at 4 weeks, cell viability is still maintained in both PDLLA-PEG 1000 and PLLA-PEG 1000 (Figure S1). We hypothesize that the material PLLA-PEG 1000 performs poorly in both ECM production and gene expression because of limited diffusion due to the L configuration of the lactide molecules which does not allow water to move through and penetrate the scaffold as readily as in the PDLLA scaffolds, which is reflected in its slower degradation than PDLLA.[42] This property would potentially lead to decreased nutrient diffusion and a smaller “space” sensed by cells, thus magnifying the polymer concentration effect on matrix production. While Bryant et al. previously noted that in non-degradable and partially degrading PEG networks ECM production did not vary within a range of about 1 MPa and 10-30% w/w concentration[39], our hydrogels are fully degradable and thus lend a different microenvironment. Our observations also contrast with the study by Bian et al., which demonstrated that higher crosslinking densities decreased cartilage ECM production.[31] This discrepancy, however, can be reconciled by their observation that higher crosslinking density actually resulted in higher concentrations of hyaluronic acid retained in the material. Thus, by viewing these findings in terms of decreased cell space rather than increased crosslinking density, they are consistent with our observations and conclusions.

While ECM production is one measure of efficacy, one of the main limitations of our study is that none of the scaffolds were able to achieve our end goal of constructs that can retain mechanical strength over time. On examination of histological sections (Figure 7), we see that even in the groups with adequate nutrient diffusion, the deposited ECM is localized only around cell clusters and not distributed within the PEG material (holes seen in the material are due to sample processing). This localized distribution of ECM has been observed in other studies utilizing PEG-based materials as well[38,39], and is a likely cause to the inability of the deposited ECM to reinforce the scaffold. Indeed, studies utilizing high cell concentrations allowing for cell contact, materials that result in distributed ECM deposition within the scaffold, or cell pellets all have demonstrated the ability to increase mechanical strength over time – albeit starting from a low mechanical strength[20,43–46]. In addition to lack of mechanical property retention, another limitation lies in the appearance of hypertrophic cells, a well-known shortcoming of MSC chondrogenesis in 3D scaffolds. Based on expression levels of hypertrophy related genes MMP13 and ColX (Figure 6) the new material PDLLA-PEG 1000 is not able to reduce hypertrophic response, an inevitable consequence of exposure to TGF-β3 containing chondroinductive medium.[47,48] However, it does offer the advantage of increased mechanical strength without a decrease in ECM production.

Overall, we have established here an optimal cell seeding density and introduced a new material, PDLLA-PEG 1000, that is similarly pro-chondrogenic for encapsulated BMSCs as the PDLLA-PEG 4000 we previously reported, and we have demonstrated that within the 150 kPa – 1500 kPa range, material concentration plays an important role in determining cellular response rather than material stiffness or crosslinking density. This new material also exhibits substantially improved mechanical strengths approximately 4 times higher than its high molecular weight counterpart after 4 weeks of culture. However, the mechanical strength of the PDLLA-PEG 1000 scaffold is still not adequately augmented by new ECM produced by the seeded cells. Given the absence of cell-binding sites on PDLLA-PEG, it is possible that the supplementation of molecules that can interact with cells, such as hyaluronic acid, can aid in ECM deposition and crosslinking.[49–51] Another challenge is the limited nutrient diffusion into the biomaterial scaffold. Mauck et al. previously showed that mechanical loading increases nutrient diffusion through hydrogels and improves mechanical properties of agarose scaffolds after 4 weeks of cyclic loading, and allows for cell densities higher than 20×10^6 cells/mL to be optimal.[52,53] A similar mechanical regimen may be tested here. Lastly, increasing the PDLLA to PEG ratio in our polymers may allow for increased cell contact and ECM crosslinking due to increased “space” due to higher rates of degradation. These concepts will be tested to achieve a cell incorporated construct that can retain mechanical properties for cartilage tissue engineering.

5. Conclusion

In this study, we have determined that BMSC seeding at 20×10^6 cells/mL allows for optimal efficiency of ECM production per cell for cell incorporated PDLLA-PEG hydrogels in static culture. We also conclude that within the physiological range of cartilage mechanical properties in PDLLA-PEG hydrogels, material concentration but not material stiffness influences cell ability to secrete ECM with increasing hydrogel concentrations

limiting matrix deposition. This characteristic implies that degradable PEG hydrogels that possess high stiffness at low polymer concentrations are better able to maximize cell free space concurrently with mechanical strengths and would be optimal for cartilage tissue engineering. Lastly, we have introduced a new material, PDLLA-PEG 1000, that possesses mechanical strength in the physiologic range of native cartilage and strong chondrogenic potential. Our current work aims to optimize and develop this material for the repair of cartilage defects in future studies.

Supplementary Material

Refer to Web version on PubMed Central for supplementary material.

Acknowledgments

The authors gratefully thank Dr. Paul Manner (University of Washington) for providing tissue, Dr. Jian Tan (University of Pittsburgh) for isolating hBMSCs, and Dr. Guang Yang for creating the graphical abstract. This work is supported in part by the National Institutes of Health (R01 EB019430 and T32 GM008208) and the U.S. Department of Defense (W81XWH-14-1-0217). Aaron Sun is supported in part by the NIH Cellular Approaches to Tissue Engineering and Regeneration Training Grant (T32 EB001026). Dr. He Shen thanks the National Natural Science Foundation of China (81501074) and China Postdoctoral Science Foundation (2015M571836).

References

1. Tuan RS, Chen AF, Klatt BA. Cartilage regeneration. J Am Acad Orthop Surg. 2013; 21(5):303–311. [PubMed: 23637149]
2. Neogi T, Zhang Y. Epidemiology of osteoarthritis. Rheum Dis Clin North Am. 2013; 39(1):1–19. [PubMed: 23312408]
3. Bitton R. The economic burden of osteoarthritis. Am J Manag Care. 2009; 15(8 Suppl):S230–S235. [PubMed: 19817509]
4. Ye K, Di Bella C, Myers DE, Choong PFM. The osteochondral dilemma: Review of current management and future trends. ANZ J Surg. 2014; 84(4):211–217. [PubMed: 23458285]
5. Moran CG, Horton TC. Total knee replacement: the joint of the decade. A successful operation, for which there's a large unmet need. BMJ. 2000; 320(7238):820. [PubMed: 10731156]
6. Nashi N, Hong CC, Krishna L. Residual knee pain and functional outcome following total knee arthroplasty in osteoarthritic patients. Knee Surg Sports Traumatol Arthrosc. 2014:1841–1847. [PubMed: 24549262]
7. Demoor M, Ollitrault D, Gomez-Leduc T, et al. Cartilage tissue engineering: Molecular control of chondrocyte differentiation for proper cartilage matrix reconstruction. Biochim Biophys Acta - Gen Subj. 2014; 1840(8):2414–2440.
8. Kon E, Filardo G, Di Martino A, Marcacci M. ACI and MACI. J Knee Surg. 2012; 25(1):17–22. [PubMed: 22624243]
9. Dewan AK, Gibson MA, Elisseeff JH, Trice ME. Evolution of autologous chondrocyte repair and comparison to other cartilage repair techniques. Biomed Res Int. 2014; 2014:272481. [PubMed: 25210707]
10. Kuo CK, Li WJ, Mauck RL, Tuan RS. Cartilage tissue engineering: its potential and uses. Curr Opin Rheumatol. 2006; 18(1):64–73. [PubMed: 16344621]
11. Pittenger MF. Multilineage potential of adult human mesenchymal stem cells. Science. 1999; 284(5411):143–147. [PubMed: 10102814]
12. Rodríguez-merchán EC. Intra-articular injections of mesenchymal stem cells for knee osteoarthritis. Am J Orthop. 2014; 43(12):282–291.
13. Emadedin M, Aghdami N, Taghiyar L, et al. Intra-articular injection of autologous mesenchymal stem cells in six patients with knee osteoarthritis. Arch Iran Med. 2012; 15(7):422–428. [PubMed: 22724879]

14. Jo CH, Lee YG, Shin WH, et al. Intra-articular injection of mesenchymal stem cells for the treatment of osteoarthritis of the knee: A proof-of-concept clinical trial. Stem Cells. 2014; 32(5): 1254–1266. [PubMed: 24449146]
15. Li K-C, Hu Y-C. Cartilage tissue engineering: recent advances and perspectives from gene regulation/therapy. Adv Healthc Mater. 2015; 4(7):948–68. [PubMed: 25656682]
16. Bhardwaj N, Devi D, Mandal BB. Tissue-engineered cartilage: The crossroads of biomaterials, cells and stimulating factors. Macromol Biosci. 2015; 15(2):153–182. [PubMed: 25283763]
17. Trzeciak T, Richter M, Suchorska W. Application of cell and biomaterial-based tissue engineering methods in the treatment of cartilage, menisci and ligament injuries. 2016. Int Orthop. 2016; 40(3): 615–624. [PubMed: 26762517]
18. Sun AX, Lin H, Beck AM, Kilroy EJ, Tuan RS. Projection stereolithographic fabrication of human adipose stem cell-incorporated biodegradable scaffolds for cartilage tissue engineering. Front Bioeng Biotechnol. 2015 Aug.3:115. [PubMed: 26347860]
19. Huang AH, Stein A, Tuan RS, Mauck RL. Transient exposure to transforming growth factor beta 3 improves the mechanical properties of mesenchymal stem cell-laden cartilage constructs in a density-dependent manner. Tissue Eng Part A. 2009; 15(11):3461–3472. [PubMed: 19432533]
20. Erickson IE, Kestle SR, Zellars KH, et al. High mesenchymal stem cell seeding densities in hyaluronic acid hydrogels produce engineered cartilage with native tissue properties. Acta Biomater. 2012; 8(8):3027–3034. [PubMed: 22546516]
21. Ponticiello MS, Schinagl RM, Kadiyala S, Barry FP. Gelatin-based resorbable sponge as a carrier matrix for human mesenchymal stem cells in cartilage regeneration therapy. J Biomed Mater Res. 2000; 52(2):246–255. [PubMed: 10951362]
22. Kavalkovich KW, Boynton RE, Murphy JM, Barry F. Chondrogenic differentiation of human mesenchymal stem cells within an alginate layer culture system. In Vitro Cell Dev Biol Anim. 2002; 38(8):457–466. [PubMed: 12605540]
23. Engler AJ, Sen S, Sweeney HL, Discher DE. Matrix elasticity directs stem cell lineage specification. Cell. 2006; 126(4):677–689. [PubMed: 16923388]
24. Tse JR, Engler AJ. Stiffness gradients mimicking in vivo tissue variation regulate mesenchymal stem cell fate. PLoS One. 2011; 6(1):e15978. [PubMed: 21246050]
25. Kshitiz, Park J, Kim P, et al. Control of stem cell fate and function by engineering physical microenvironments. Integr Biol (Camb). 2012; 4(9):1008–1018. [PubMed: 23077731]
26. Khetan S, Guvendiren M, Legant WR, Cohen DM, Chen CS, Burdick JA. Degradation-mediated cellular traction directs stem cell fate in covalently crosslinked three-dimensional hydrogels. Nat Mater. 2013; 12(5):458–465. [PubMed: 23524375]
27. Yang C, Tibbitt MW, Basta L, Anseth KS. Mechanical memory and dosing influence stem cell fate. Nat Mater. 2014; 13(6):645–652. [PubMed: 24633344]
28. Murphy WL, McDevitt TC, Engler AJ. Materials as stem cell regulators. Nat Mater. 2014; 13(6): 547–557. [PubMed: 24845994]
29. Wen JH, Vincent LG, Fuhrmann A, et al. Interplay of matrix stiffness and protein tethering in stem cell differentiation. Nat Mater. 2014; 13:979–987. [PubMed: 25108614]
30. Hendriks JAA, Moroni L, Riesle J, de Wijn JR, van Blitterswijk CA. The effect of scaffold-cell entrapment capacity and physico-chemical properties on cartilage regeneration. Biomaterials. 2013; 34(17):4259–4265. [PubMed: 23489921]
31. Bian L, Hou C, Tous E, Rai R, Mauck RL, Burdick JA. The influence of hyaluronic acid hydrogel crosslinking density and macromolecular diffusivity on human MSC chondrogenesis and hypertrophy. Biomaterials. 2013; 34(2):413–421. [PubMed: 23084553]
32. Toh WS, Lim TC, Kurisawa M, Spector M. Modulation of mesenchymal stem cell chondrogenesis in a tunable hyaluronic acid hydrogel microenvironment. Biomaterials. 2012; 33(15):3835–3845. [PubMed: 22369963]
33. Caterson EJ, Nesti LJ, Danielson KG, Tuan RS. Human marrow-derived mesenchymal progenitor cells: isolation, culture expansion, and analysis of differentiation. Mol Biotechnol. 2002; 20(3): 245–256. [PubMed: 11936255]

34. Seck TM, Melchels FPW, Feijen J, Grijpma DW. Designed biodegradable hydrogel structures prepared by stereolithography using poly(ethylene glycol)/poly(d,l-lactide)-based resins. J Control Release. 2010; 148(1):34–41. [PubMed: 20659509]
35. Fairbanks BD, Schwartz MP, Bowman CN, Anseth KS. Photoinitiated polymerization of PEG-diacrylate with lithium phenyl-2,4,6-trimethylbenzoylphosphinate: polymerization rate and cytocompatibility. Biomaterials. 2009; 30(35):6702–6707. [PubMed: 19783300]
36. Safranski DL, Gall K. Effect of chemical structure and crosslinking density on the thermo-mechanical properties and toughness of (meth)acrylate shape memory polymer networks. Polymer (Guildf). 2008; 49(20):4446–4455.
37. Sawhney, Amarprett S., Handrashokher, C., Pathak, P., H, JA. Bioerodible hydrogels based on photopolymerized poly(ethy1eneglycol)-co-poly(a-hydroxy acid) diacrylate macromers. Macromolecules. 1993; 26:581–587.
38. Bryant SJ, Anseth KS. Controlling the spatial distribution of ECM components in degradable PEG hydrogels for tissue engineering cartilage. J Biomed Mater Res A. 2003; 64(1):70–79. [PubMed: 12483698]
39. Bryant SJ, Anseth KS. Hydrogel properties influence ECM production by chondrocytes photoencapsulated in poly(ethylene glycol) hydrogels. J Biomed Mater Res. 2002; 59(1):63–72. [PubMed: 11745538]
40. Ikada Y. Challenges in tissue engineering. J R Soc Interface. 2006; 3(10):589–601. [PubMed: 16971328]
41. Farrell MJ, Comeau ES, Mauck RL. Mesenchymal stem cells produce functional cartilage matrix in three-dimensional culture in regions of optimal nutrient supply. Eur Cell Mater. 2012; 23:425–440. [PubMed: 22684531]
42. Li WJ, Cooper JA, Mauck RL, Tuan RS. Fabrication and characterization of six electrospun poly(α-hydroxy ester)-based fibrous scaffolds for tissue engineering applications. Acta Biomater. 2006; 2(4):377–385. [PubMed: 16765878]
43. Levett PA, Melchels FPW, Schrobback K, Hutmacher DW, Malda J, Klein TJ. A biomimetic extracellular matrix for cartilage tissue engineering centered on photocurable gelatin, hyaluronic acid and chondroitin sulfate. Acta Biomater. 2014; 10(1):214–223. [PubMed: 24140603]
44. Tuli R, Nandi S, Li WJ, et al. Human mesenchymal progenitor cell-based tissue engineering of a single-unit osteochondral construct. Tissue Eng. 2004; 10(7–8):1169–1179. [PubMed: 15363173]
45. Bhumiratana S, Eton RE, Oungoulian SR, Wan LQ, Ateshian GA, Vunjak-Novakovic G. Large, stratified, and mechanically functional human cartilage grown in vitro by mesenchymal condensation. Proc Natl Acad Sci U S A. 2014; 111(19):6940–6945. [PubMed: 24778247]
46. Bian L, Guvendiren M, Mauck RL, Burdick JA. Hydrogels that mimic developmentally relevant matrix and N-cadherin interactions enhance MSC chondrogenesis. Proc Natl Acad Sci U S A. 2013; 110(25):10117–10122. [PubMed: 23733927]
47. Hubka KM, Dahlin RL, Meretoja VV, Kasper K, Mikos AG. Enhancing chondrogenic phenotype for cartilage tissue engineering: monoculture and co-culture of articular chondrocytes and mesenchymal stem cells. Tissue Eng Part B. 2014; 20(6):1–50.
48. Chen S, Fu P, Cong R, Wu HS, Pei M. Strategies to minimize hypertrophy in cartilage engineering and regeneration. Genes Dis. 2015; 2(1):76–95. [PubMed: 26000333]
49. Bian L, Guvendiren M, Mauck RL, Burdick JA. Hydrogels that mimic developmentally relevant matrix and N-cadherin interactions enhance MSC chondrogenesis. Proc Natl Acad Sci U S A. 2013; 110(25):10117–10122. [PubMed: 23733927]
50. Klein TJ, Rizzi SC, Schrobback K, et al. Long-term effects of hydrogel properties on human chondrocyte behavior. Soft Matter. 2010; 6:5175.
51. Chung C, Burdick JA. Influence of three-dimensional hyaluronic acid microenvironments on mesenchymal stem cell chondrogenesis. Tissue Eng Part A. 2009; 15(2):243–254. [PubMed: 19193129]
52. Mauck RL, Wang CCB, Oswald ES, Ateshian GA, Hung CT. The role of cell seeding density and nutrient supply for articular cartilage tissue engineering with deformational loading. Osteoarthr Cartil. 2003; 11(12):879–890. [PubMed: 14629964]

53. Mauck RL, Seyhan SL, Ateshian GA, Hung CT. Influence of Seeding Density and Dynamic Deformational Loading on the Developing Structure/Function Relationships of Chondrocyte-Seeded Agarose Hydrogels. Ann Biomed Eng. 2002; 30(8):1046–1056. [PubMed: 12449765]

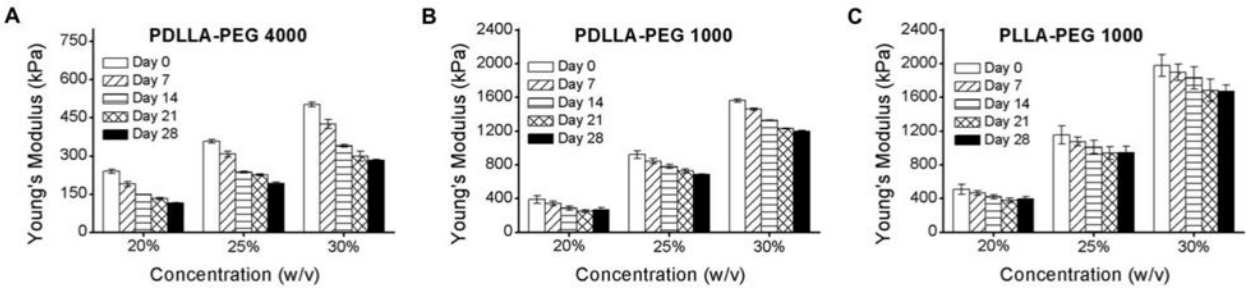

Figure 1. Mechanical properties and degradation of polymers as a function of polymer concentrations and incubation time

(A) PDLLA-PEG 4000; (B) PDLLA-PEG 1000; and (C) PLLA-PEG 1000. Statistically significant reductions in compressive moduli are seen at each increasing time point ($p<0.001$) and each concentration for all materials, except between days 21 and 28 where $p > 0.5$. In addition, the main effects of material type and material concentration are significantly different for these biomaterials ($p<0.001$ based on two-way independent ANOVA). n = 3 replicates for all groups.

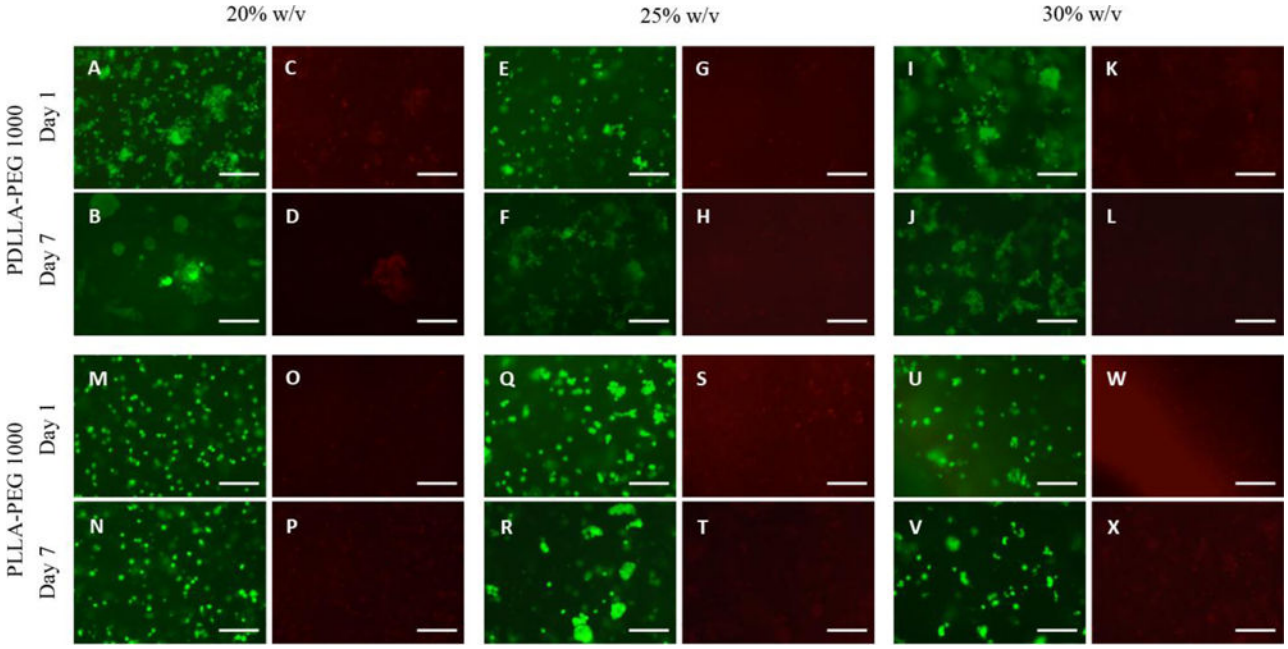

Figure 2. Cell viability in hydrogel constructs

(A,B,E,F,I,J,M,N,Q,R,U,V) Calcein-AM staining (green, live cells) and **(C,D,G,H,K,L,O,P,S,T,W,X)** EthD-1 staining (red, dead cells) in cell-seeded scaffolds following fabrication at days 1 and 7 across 20%, 25%, and 30% w/v polymer concentrations. Cell viability at day 7 was >85% in all groups based on green count/ total count. Scale bar = 150 μm.

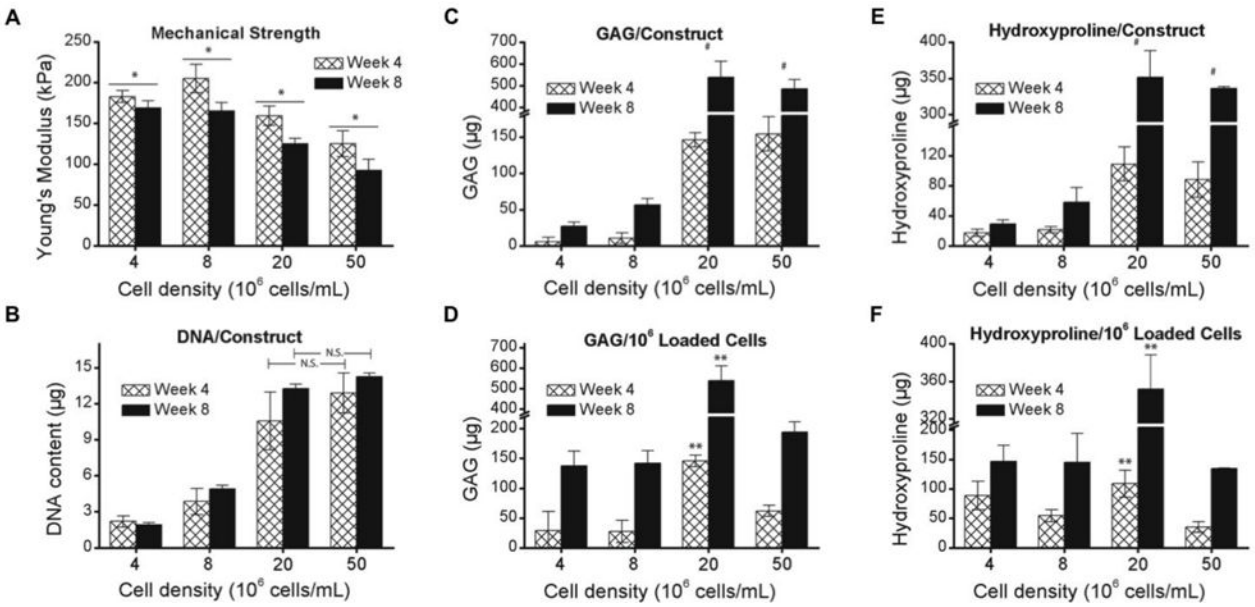

Figure 3. Effect of cell density on ECM synthesis

BMSCs were seeded in 30% PDLLA-PEG 4000 at densities ranging from 4 - 50 × 10^6 cells/mL. **(A)** Mechanical strength of constructs after 4 and 8 weeks of static culture. **(B)** Total cell number estimated from DNA content in constructs **(C,E)** Total ECM deposition measured by **(C)** GAG and **(E)** Hydroxyproline contents per construct. **(D,F)** ECM deposition normalized to initial cell loading number. *, $p<0.05$, between week 4 and week 8. #, $p<0.001$, for 20 and 50 × 10^6 cells/mL groups *versus* 4 and 8 × 10^6 cells/mL groups at both timepoints, and no significant difference between 20 and 50 × 10^6 cells/mL. **, $p<0.001$, when compared to all other groups at the same time point. n = 6 replicates per group.

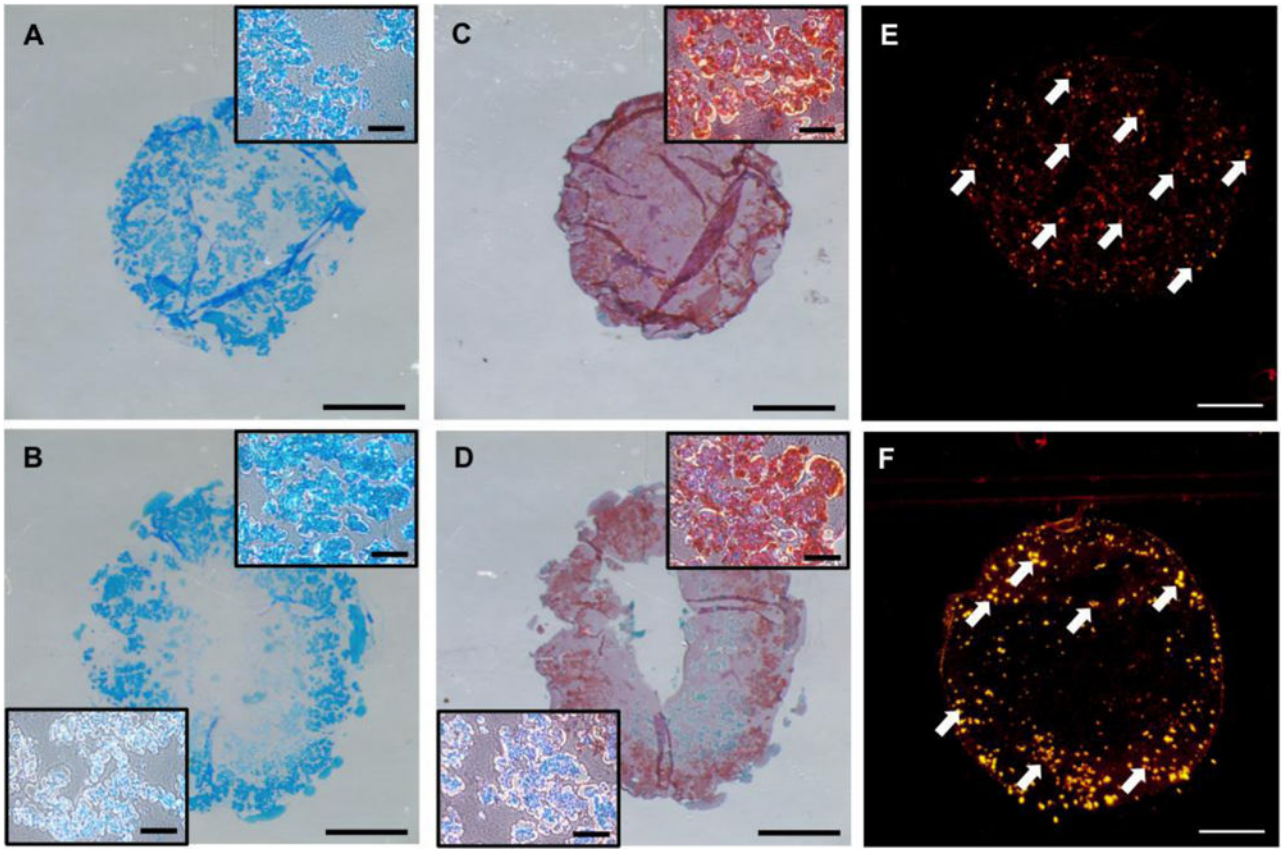

Figure 4. ECM deposition in high cell density constructs at 8 weeks

(A,C) Macroscopic view of **(A)** Alcian Blue/Fast Red staining and **(C)** Safranin O/fast green staining for GAG deposition in 20×10^6 cells/mL. Inset is a higher magnification representative region in the construct. **(B,D)** Macroscopic view of **(B)** Alcian Blue/Fast Red and **(D)** Safranin O/Fast Green staining at 50×10^6 cells/mL. Top right inset is higher magnification representative region in periphery of construct while bottom left shows higher magnification representative region in more central zone of the construct. **(E,F)** Cellular uptake of fluorescently labeled transferrin at 20×10^6 cells/mL and 50×10^6 cells/mL after 14 days of static culture, respectively. Scale bars = 1500 μm in macroscopic views, 150 μm in the insets.

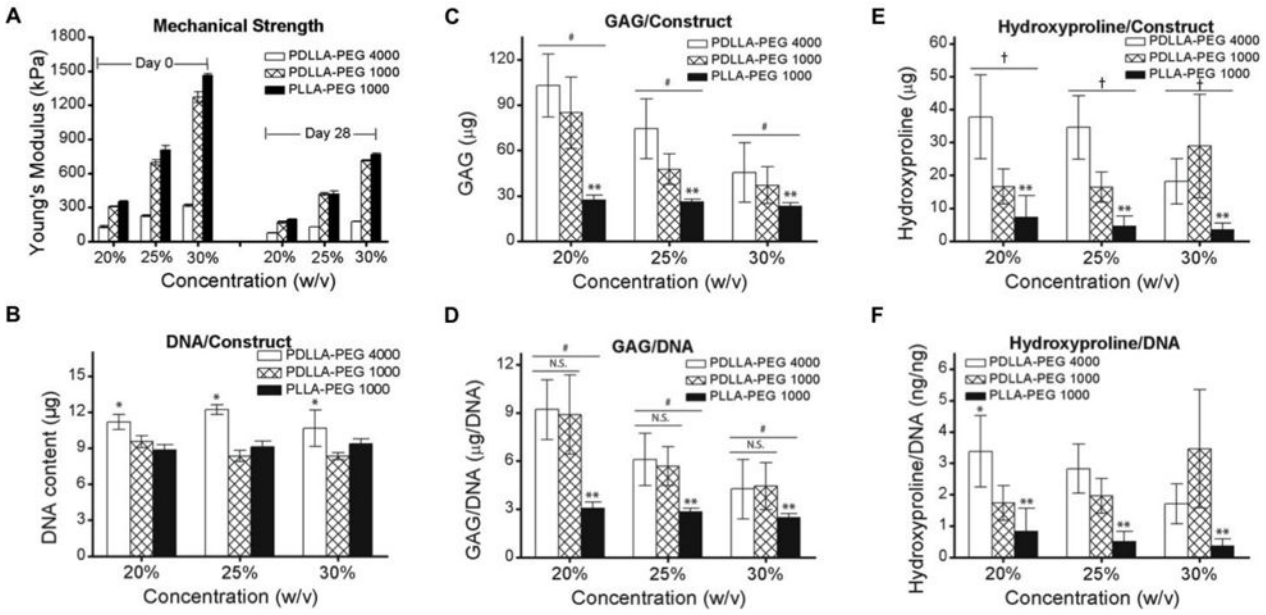

Figure 5. Effect of material concentration and stiffness on ECM deposition

BMSCs were seeded at 20 × 10^6 cells/mL in scaffolds of different polymer concentrations and material properties. **(A)** Mechanical strength post fabrication and after 4 weeks of culture. Mechanical properties of PDLLA and PLLA-PEG 1000 were significantly higher at all polymer concentrations and timepoints than corresponding PDLLA-PEG 4000 ($p<0.001$). **(B)** Cell number measured on the basis of DNA content in constructs. **(C,E)** Total ECM deposition measured by **(C)** GAG and **(E)** Hydroxyproline production per construct. **(D, F)** ECM deposition normalized to DNA content. *, $p<0.001$, as compared to other materials at same concentration. **, $p<0.001$, for main effect of material as compared to others. #, $p<0.05$, for main effect of material concentration between concentrations and $p<0.005$ for main effect of PDLLA-PEG 4000 *versus* other groups. †, $p<0.005$, for main effect of PDLLA-PEG 4000 *versus* other groups. All effects were determined by Tukey's HSD post-hoc testing following two-way independent ANOVA analysis. n = 6 replicates per group.

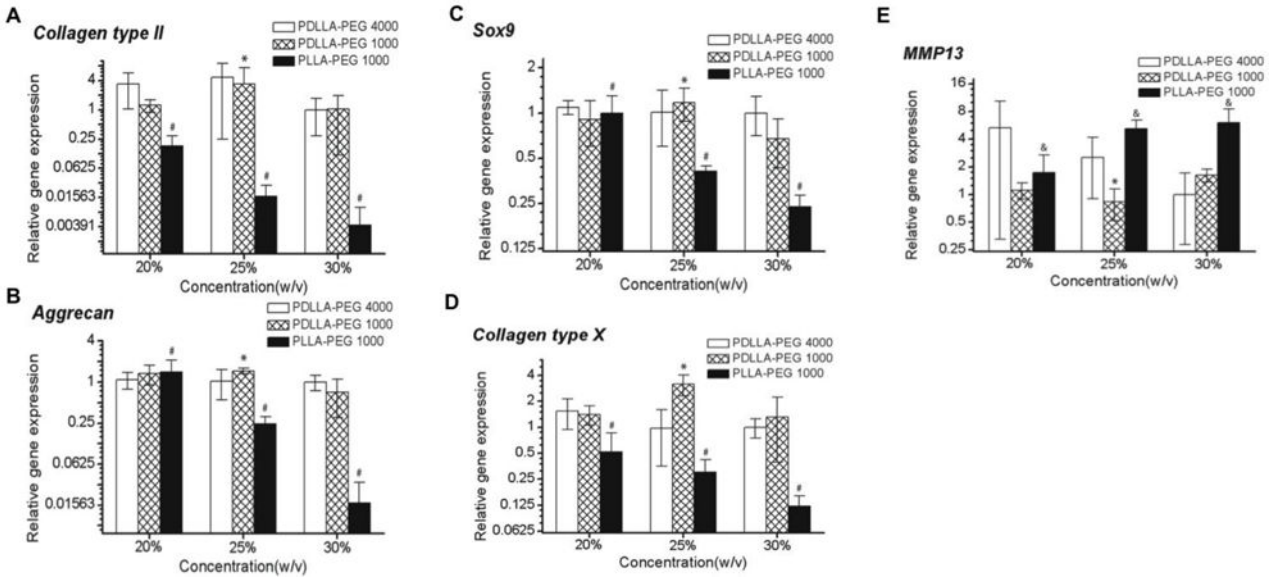

Figure 6. Real-time PCR analysis of gene expression in hBMSC seeded constructs (20×10^6 cells/mL) at day 28

Relative gene expression levels of **(A)** collagen type II, **(B)** Aggrecan, **(C)** Sox9, **(D)** collagen type X, and **(E)** MMP13, normalized to cell gene expression in PDLLA-PEG 4000 at 30% w/v polymer concentration. Overall, two-way independent MANOVA analysis of PDLLA-PEG 4000 *versus* 1000 revealed no significant differences across all genes except MMP13 ($p=0.027$). *, $p<0.05$, for PDLLA-PEG 1000 25% *versus* 30%. #, $p< 0.005$, between all concentrations for PLLA-PEG 1000 except collagen type X, where 20% *versus* 25% showed $p=0.286$. &, $p<0.005$, between 20% *versus* 25% and 30%. n = 6 replicates per group.

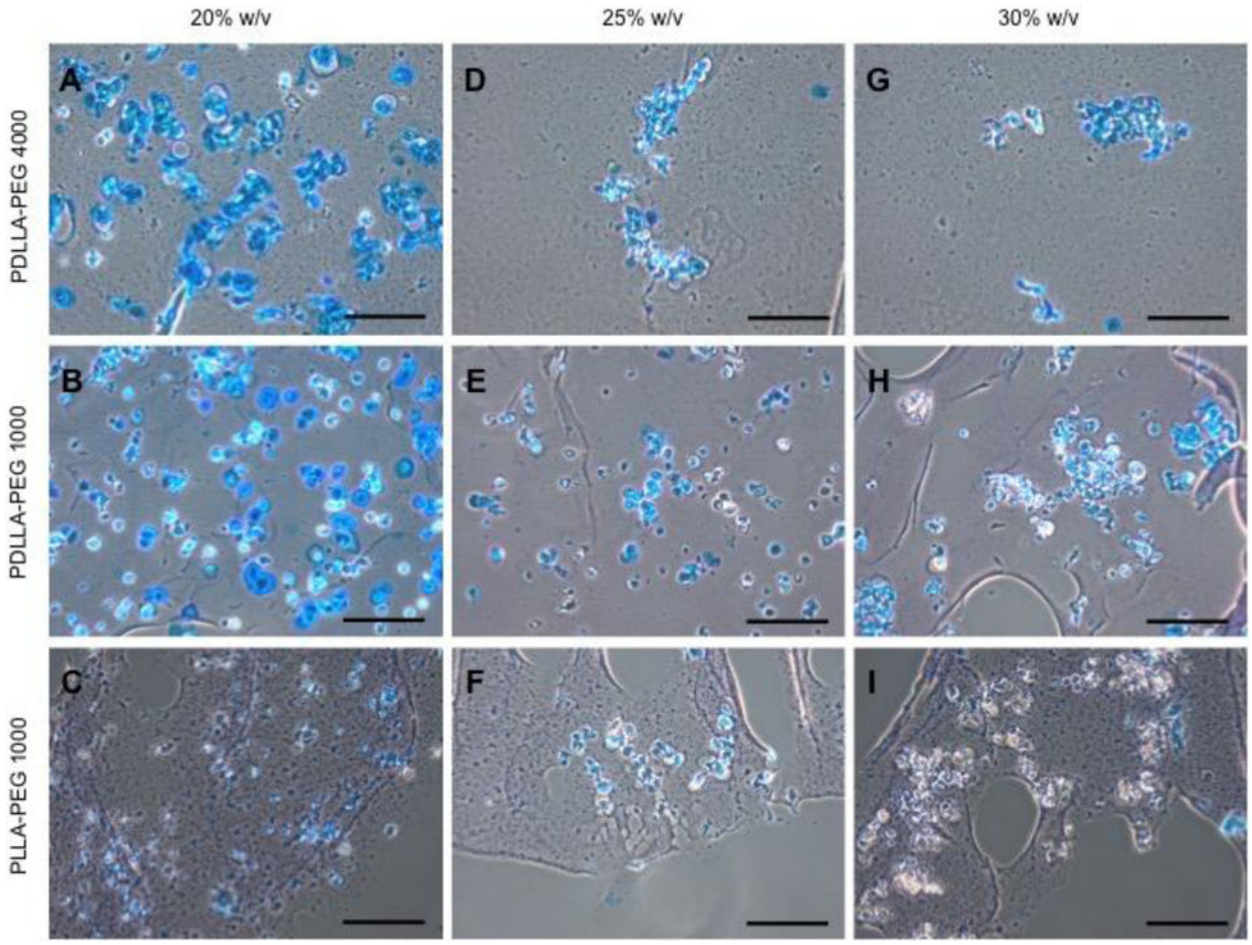

Figure 7. Glycosaminoglycan content in hBMSC-encapsulated constructs (20×10^6 cells/mL) visualized by Alcian Blue/Fast Green staining at day 28

(A,D,G) Staining of PDLLA-PEG 4000 group. **(B,E,H)** Staining of PDLLA-PEG 1000 group. **(C,F,I)** Staining of PLLA-PEG 1000. Scale bar = 150 μm. Center of scaffold is towards top left of images, and images were obtained between the center and edge of scaffold.